energies

MDPI

Article

A Feasibility Study of Frequency Regulation Energy Storage System Installation in a Power Plant

Lateef Onaadepo Ibrahim [1], Youl-Moon Sung [1], Doosoo Hyun [2] and Minhan Yoon [3,*]

[1] Department of Electrical Engineering, Kyungsung University, Busan 48434, Korea; jakande8051@ks.ac.kr (L.O.I.); ymsung@ks.ac.kr (Y.-M.S.)
[2] Department of Electrical Engineering, Dongyang Mirae University, Seoul 08221, Korea; dshyun@dongyang.ac.kr
[3] Department of Electrical Engineering, Kwangwoon University, Seoul 01897, Korea
* Correspondence: minhan.yoon@gmail.com; Tel.: +82-2-940-5108

Received: 30 August 2020; Accepted: 9 October 2020; Published: 15 October 2020

Abstract: The aim of this work is to analyze and stabilize the power system when connecting an energy storage system (ESS) to replace the traditional power reserve of a power plant. Thus, it is necessary to validate and simulate the power facility protection system using a relay coordination approach. The input feasibility of the generator for the frequency regulation (FR) of the operational ESS is also validated through detailed analysis studies including power flow, short circuit and relay coordination analysis. The case scenarios for ESS installation are categorized based on its operation mode and location in the power system. These studies are carried out on the power system at the peak load condition specified for both grids. With the electrical transient analyzer program (ETAP), an analysis is performed to study the implementation of the ESS in a large, integrated power system to determine which location best fits the installation of ESS considering the load flow, short circuit and relay coordination results in each case scenario. Cost evaluation was performed for the choice of locations under study.

Keywords: ESS location; ESS operation; short circuit; load flow; ESS; relay coordination; ETAP

1. Introduction

Energy storage systems (ESSs) offer technical, economic and environmental benefits in power systems; thus, their implementation in distribution networks has increased. These benefits include power quality improvement, frequency regulation, the mitigation of voltage deviation, the facilitation of renewable energy source (RES) integration, power network expansion and overall cost reduction, among others. In [1,2], the author highlighted the technical benefits of ESS usage, including reduced power losses, utility system reliability for energy sustainability, improved power and voltage quality and reduced distribution congestion. In a power system, energy storage can be used in three different modes: charge, store and discharge. In each of these modes, a balance between power and energy must be maintained. Thus, the energy storage needs to have an appropriate rated power and energy capacity [3]. Thus, this represents essential equipment that provides an attractive means of restoring the balance between power demand and supply. Energy storage has played a major role in reducing electricity costs by storing electricity obtained in off-peak periods for use at peak times instead of incurring higher costs [4,5]. In order to improve the reliability of the power supply, an ESS supports users when power network failures occur due to natural disasters. It also serves the role of improving and maintaining power quality frequency and voltage [6,7]. ESS has been described as the most powerful advantage for the simultaneous control of active and reactive power [8]. It has been shown that renewable energy integration, alternating current (AC) and direct current (DC) bus microgrids are

application fields of ESS [9]. Thus, this key technology has attracted a great deal of attention in power system research.

Consumers' locations are often far from power-generating facilities, which sometimes leads to a higher chance of interruption in the power supply. Therefore, the power flow in transmission grids is determined by the supply and demand of electricity, which necessitates the establishment of an ESS at appropriate sites. In order to maximize the benefits from an ESS operation, it is important to determine the optimal ESS location in a power network. An ESS may be installed at different voltage levels and/or locations in a power system. It may be installed close to a generation unit or at the consumers' end, depending on the size and application; for instance, installation can be completed close to the consumer in load leveling or power backup, and installation can be completed close to the generator to level the generated power by renewable energy sources [10].

An important assessment to be made to balance technical and economic factors is the optimal sizing of an ESS. The appropriate sizing of an ESS facility is important for its economic operations. An oversized ESS is not economical due to the excess capital costs which may be incurred, while an undersized ESS does not meet storage capacity requirements [10,11].

In this paper, the modeling of an ESS is required to investigate the installation of an ESS based on its operation mode and location in the power system. ESS models consist of power electronic converters which behave as positive/negative constant power loads (CPLs). A typical example of a CPL is a DC/AC inverter. In CPLs, the input voltage increases/decreases when the input current decreases/increases [12]. Power system analysis studies are performed for each case scenario to achieve the best position for the installation of the ESS.

A protection system is essential for a power system in order to minimize damage and ensure that supply is in an economically and continuously safe condition; thus, a reliable and efficient protection scheme must be provided [13]. Relay coordination study helps to determine the proper settings for overcurrent protective devices in the power system. To determine these settings, overcurrent relays (OCRs) are plotted on time–current curve (TCC) graphs [14]. When existing equipment is replaced with higher rated equipment or an existing power system is modified by installing new loads, it is necessary to conduct a coordination study [15].

In this paper, we propose a software approach for the investigation of ESS installation positions by considering the ESS's capacity size and the power grid under peak load conditions. Using the proposed method, the modeling of the power plant can be achieved while the implementation of the software provides a comprehensive analysis of the result in report formats. The alert function of the load flow and short circuit modules of the electrical transient analyzer program (ETAP) represent a convenient way to size protective devices at the facility.

2. System Description

2.1. On-Site Power System Modeling

The power system is designed using the electrical transient analyzer program (ETAP) software (ETAP: version 19, OTI, Irvine, CA, USA). The power is provided to the system by two independent sources—the 345 kV Power Grid A and 154 kV sub-station—each with a peak load condition of 40 GVAsc short circuit capacity, X/R (10) and 8149.58 MVAsc short circuit capacity, X/R (30.91141), respectively. There are two units—unit A and unit B—at the 345 kV side of the power system, each consisting of a main transformer (345 kV/22 kV), generator (612 MVA) and auxiliary transformer (53.5/26.65/26.65 (FA) MVA). The 154 kV sub-station consists of a start-up transformer (40/20/20 MVA). Protective devices—mainly overcurrent relays (OCRs), current transformer (CTs), potential transformer (PTs) and circuit breakers (CBs)—are connected according to design specifications. The loads, which are mainly induction machines, are connected to the low-voltage bus level (6.9 kV) with a load sum of 25 MW installed capacity. The power factors (PFs) considered for these induction machines vary with loads, which are specified as 100% (full) load, 75% load and 50% load with no load conditions. The PFs

range from 0.82~0.93 at full load, 0.80~0.92 at 75% load and 0.688~0.875 at 50% load. The efficiency of these machines are also specified in terms of 100%, 75%, 50% load and no load. In order to avoid analysis error in the modeling, the start-up transformer's circuit breakers in the 154 kV unit system should be in an open state. The entire power system model one-line diagram is shown in Figure 1.

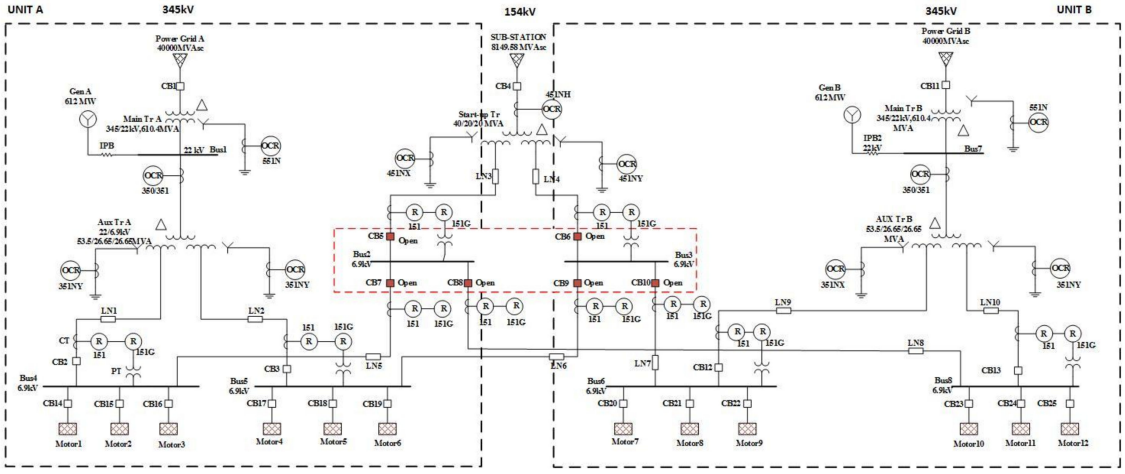

Figure 1. Power system model one-line diagram.

2.2. Load Flow and Short Circuit Studies

Load flows, which are necessary for the planning, operation, economic scheduling and exchange of power between utilities [16,17], are performed for the power system (Figure 1) as designed and simulated using ETAP. This is done to ensure that the bus voltages are near the rated values, that the generators operate within their operating limits and that the transmission lines with associated transformers are not overloaded [18].

An unbalanced system is the result of the occurrence of a fault [19]. Thus, the maximum and minimum available fault currents need to be calculated for all busses to ensure that each component rating is adequate to withstand or interrupt the fault current. In this work, the system analysis of the power system is carried out considering the state of circuit breakers CB5, CB6, CB7, CB8, CB9 and CB10 in an open state. Circuit breakers CB5, CB7 and CB8 are located on the upper and lower part of Bus 2, while CB6, CB9 and C10 are located on the upper and lower part of Bus 3 in the 154 kV grid, as shown in Figure 1. Thus, data are used to evaluate the correct sizing of protective relays and detection equipment [20].

2.3. Overcurrent Relay Coordination

OCRs are the most common protective devices employed to counteract abnormal currents in power systems. The coordination between protection devices is established to isolate only faulty sections, meaning that the healthy section is kept energized [21]. Thus, to determine the proper setting of the overcurrent relays (OCR 151 and 151G) in the system, we plot these on the time–current characteristics curve (TCCs) graph. The coordination is performed from the 6.9 kV (downstream) voltage level to the 345 kV and 154 kV (upstream) voltage levels. The protective device setting parameters implemented in this work are summarized in Tables 1 and 2 below.

2.4. ESS Modeling

The ESS model in this work can be characterized as an equivalent impedance model in which the impedances of the ESS's internal cells, converters and transformers were considered. The total internal cells' impedance varies considerably with the state of charge (SOC), which can be related to a phase transformation. The charging and discharging of an ESS is determined by the voltage

difference between the DC voltage source and voltage over the capacitor in the converter section. Additionally, transient reactance for fault current analysis, which is the ratio of the internal generated voltage to transient current, is considered, and heat capacity was considered for the system analysis in both the maximum charge and discharge modes. In this paper, the implemented ESS uses a positive/negative constant power load (CPL). A constant power load is designed to dynamically adjust the load current inversely to the load voltage so that the load power is constant. This means that the output voltage drops when small variations occur in the current value (increasing current amount); thus, when neglecting the power dissipated into the circuit, the output power and the input power are equal [22]. In order to maintain constant power even when the voltage drops, a CPL leads to stability problems due to its tendency to increase the current [23]. Load modeling has been proven to improve the accuracy of power system analysis, which thus can be classified into static and dynamic load models. The former does not vary with time and expresses the active power (P) and reactive power (Q) as either polynomials or exponentials of voltage and frequency [23]. In this paper, a dynamic model is developed and used to verify the control method of the power system grid. The structure of the ESS is shown in Figure 2.

Table 1. Protective device parameters (overcurrent relays (OCRs)).

Protective Device	Base Current (A)	Pick-up Current (A)	Time Dial	Relay Operating Time (sec)	Plug Setting (%)	Curve Type
OCR 151	2230	2787.5	0.35	0.9	125	IEC Extremely Inverse
OCR 151G	1000	200	0.3	1.0	20	IEC Very Inverse

Table 2. Protective device parameters.

Protective Device	Current Rating	Voltage Rating
Current transformer (ratio)	3000/5 A	
Power transformer (ratio)		7200/120 V
Circuit breakers	Continuous current: 3000 A Max interrupting capability: 40 kA	7.2 kV Max Voltage

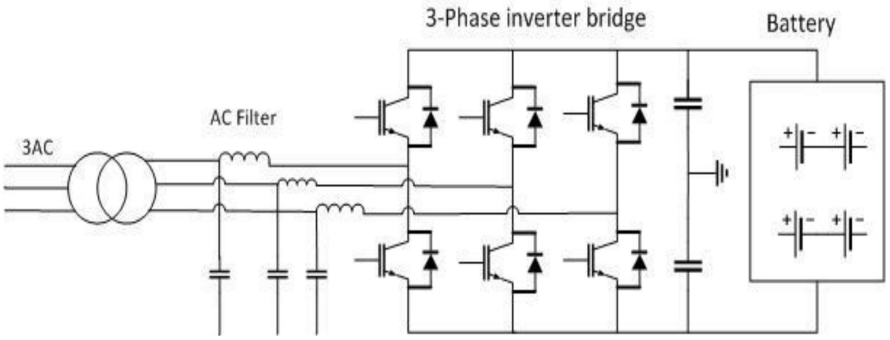

Figure 2. The structure of the energy storage system (ESS) [24].

2.5. Load Model

The dynamic load model implemented in this work is the (ZIP) model that is commonly used for both dynamic and steady-state studies and represents the relationship between the power and voltage magnitude in a polynomial equation that includes constant impedance (Z), current (I) and power (P). This study does not focus on the dynamics but on the feasibility of the application of an ESS based on static analysis, sub-transient and transient short circuit analysis and relay coordination. The sub-transient (maximum) short circuit current determines the equipment rating, while the transient (minimum) currents dictate protective device settings. A load—typically a motor—is modeled by

its positive, negative and zero sequence sub-transient and transient reactance for sub-transient and transient analysis, respectively.

2.6. ESS Installation Scenario

The scenarios that have been examined regarding the effect of the position of the ESS on the grid capabilities include cases with or without an ESS. In this paper, the feasibility studies are carried out for five cases which are based on the classification of the ESS by location and operating mode. Considering the capacity of the transformers, the case study is limited to two locations (positions 1 and 2) as shown in Figure 3. These two positions are distinguished by their respective voltage levels. Positions 1 and 2 have 6.9 kV and 22 kV bus voltage levels, respectively.

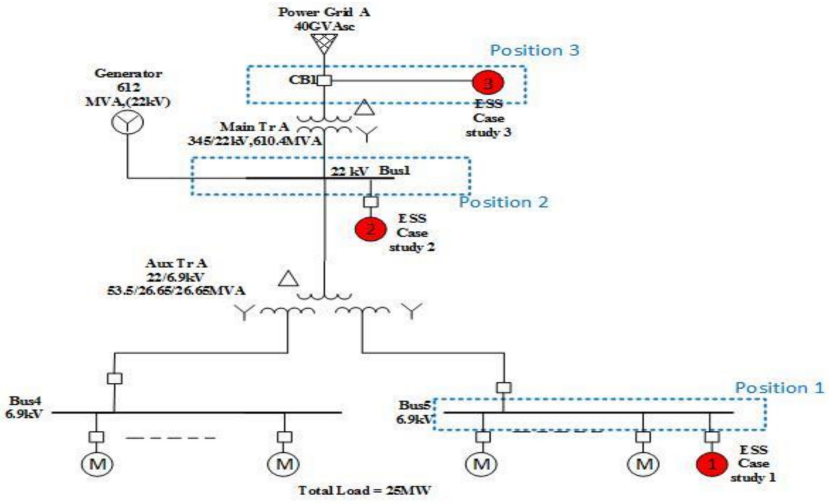

Figure 3. ESS installation case scenarios.

However, when a cost evaluation is performed for the three sites (positions 1, 2 and 3), as shown in Figure 3, position 3 can be excluded from the ESS integration to perform system analysis on the power plant. If an ESS is installed at the 345 kV stage, the current flows directly to the higher-voltage level, which is the location that has the least impact on the power plant. This necessitates an additional ultra-high-voltage substation facility. The detailed cost analysis is described in Section 3.4. The misallocation of ESSs in power networks can degrade power quality and reduce reliability as well as load control, while also affecting voltage and frequency regulation. An ESS installed at position 1, which is close to the load, has the advantage of eliminating the need to upgrade a transmission line by providing power to the end user (consumer).

ESS operating modes are classified as maximum charging (1) and maximum discharging (2). Therefore, the cases study scenarios are defined as follows:

Case 0: Without an ESS;
Case 1-1: Maximum charging operation at position 1;
Case 1-2: Maximum discharging operation at position 1;
Case 2-1: Maximum charging operation at position 2;
Case 2-2: Maximum discharging operation at position 2.

2.7. ESS Allocation Algorithm

The feasibility study of an FR-ESS based on the proposed methodologies for determining the ESS allocation in the power system is described in Section 2 in detail. As shown in Figure 4, to allocate ESS, the data of the power grid load conditions under peak conditions (e.g., the short-circuit capacity (SCC), Thevenin impedance (Zth) and reactance/resistance ratio (X/R)) as well as the generator, load

and bus have to be initialized for cases with/without an ESS. Based on this data, an ESS can be allocated following the ESS scenario described in Section 2.6. This is updated to conduct load flow, short circuit and relay coordination analyses. Given a specific ESS operation mode and location, firstly, load flow can be solved by using the accelerated gauss–seidel method. The criteria under which a condition is flagged can be provided by using a load flow study case editor, where the bus voltage (overvoltage/undervoltage) and loading of equipment (bus, transformer, generator, protective device, etc.) can be determined. If load flow is run successfully, the output is generated and analyzed; otherwise, the ESS mode data need to be verified. A three-phase fault is then applied at each bus, which generates output data when both sub-transient and transient short circuits are run. Marginal (i.e., the value is exceeded but still in a permissible state) and critical (i.e., the limit is exceeded and needs to be resolved) limits are set to flag any device which exceeds them. If the short circuit analysis is not performed, the ESS operation mode needs to be verified and updated. Under this phase fault condition, relay coordination is conducted with a star view function to verify the circuit breakers' sequence of operation. The coordinated curves (normalized TCC graph for the OCR) can be verified and set. This procedure is carried out for the power system network without an ESS and generated the results shown below.

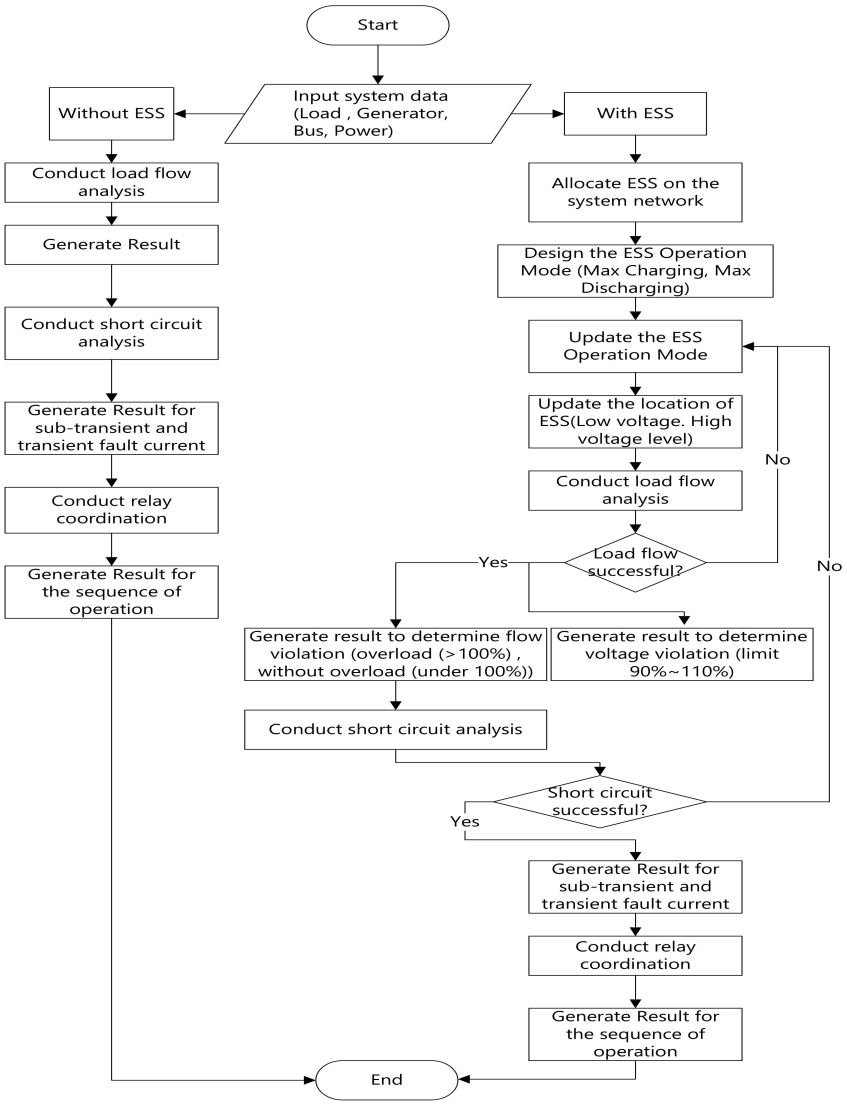

Figure 4. Flow chart of the proposed method.

3. Simulation Result and Discussion

3.1. Load Flow Study Result

The load flow analysis simulation in ETAP gives the result for the total power flow generation (MW), the total load (MW) and the active losses (MW) in each ESS installation case scenario. The total generation is the summation of the total load and the active losses. The load flow values for the summation when the power system is simulated for units A and B with the circuit breakers associated with the auxiliary transformer of the 154 kV unit in an open state is depicted in Figure 5. As shown in Figure 5a, the total generation and load for cases 1-1 and 2-1 were highest at about 100 MW and 99 MW, respectively, due to the addition of a constant load at the maximum charging operation of the ESS, while in cases 1-2 and 2-2, the generation and load were lowest at about 53 MW and 50 MW, respectively, at the maximum discharge operation of the ESS. However, the power system without an ESS installed showed about 55.5 MW and 50 MW of generation and load, respectively. The percentage losses against the total generation are plotted as shown in Figure 5b, where the lowest percentage loss was recorded for case 2-1, at about 0.022, and the highest loss in percentage was the same for case 1-2 and 2-2, at 0.051. Without an ESS, the loss was high relative to case 1-1, at about 0.047.

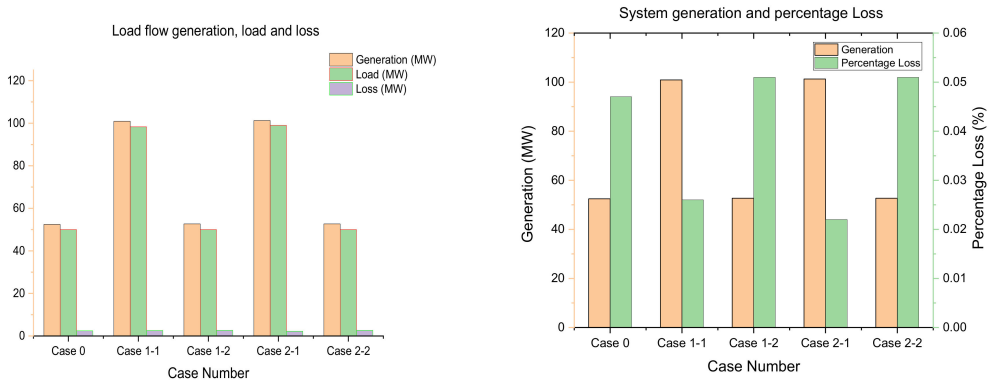

(**a**) (**b**)

Figure 5. Summation of unit A and B load flow result. (**a**) Generation, load and loss in scenarios with an ESS, (**b**) comparison of system generation with percentage loss.

The load flow data with overload (over 100%) and without overload (under 100%) are clearly depicted in Figure 6, showing the effect of the ESS operation mode to the power system. The studies show that the auxiliary transformer (tertiary winding) is overloaded for case 1-1 (maximum charging mode on 6.9 kV) at 117.5% loading, while in other case scenarios, there is no load flow violation with a transformer winding load percentage ranging from 27.4% to 73.4%, as shown in Figure 6.

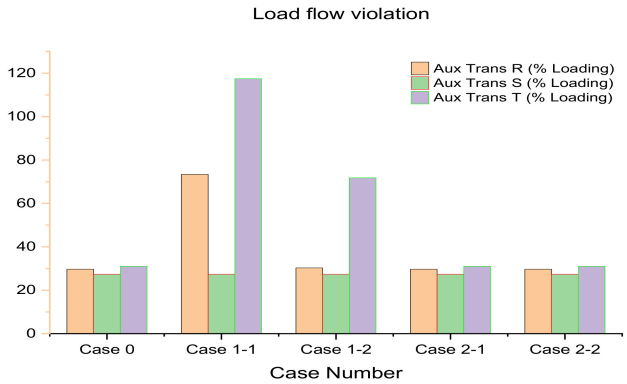

Figure 6. Load flow violation result.

The voltage range is investigated for a possible overvoltage or undervoltage violation between the ranges of 90%~110% of the nominal voltage. After employing the load flow analyzer of ETAP, the result shows that each ESS case scenario does not violate the voltage range, as depicted in Figure 7. It can be seen in Figure 7 that the percentage voltage magnitude in each case scenario has a range within 93.372% to 94.985%. The percentage magnitude of the voltage at bus 1 for the cases is about 94.985%, which is the highest, while bus 4 has a magnitude of about 93.7% and bus 5 of about 93.372%.

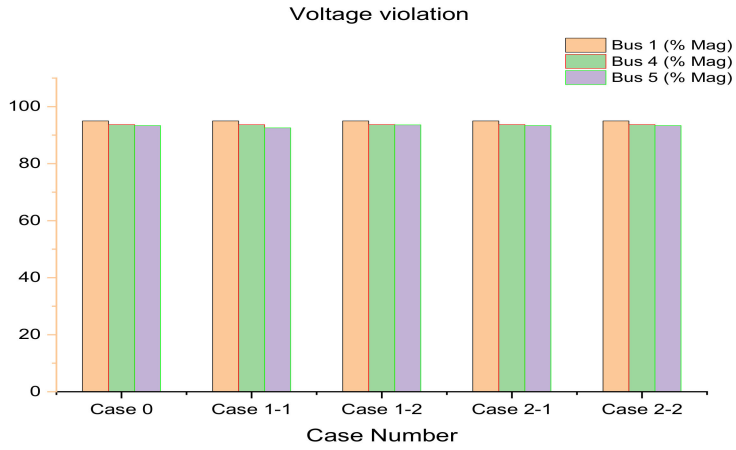

Figure 7. Voltage violation result.

3.2. Short Circuit Study Result

The power system is simulated for short circuit currents when a three-phase fault occurs on any of the busses considering each case scenario. The maximum and minimum available fault current for each bus is calculated according to the results shown in Table 3. The maximum short circuit currents are the sub-transient three-phase fault values in root-mean-square (RMS), while the minimum is the steady state transient fault current. Short circuit analysis for case 1-2 when a three-phase fault occurs at bus 5 (the bus to which the 26.65 MVA auxiliary transformer tertiary side is connected) shows that the maximum fault current of 46.836 kA has exceeded the circuit breaker's capacity of 40 kA. There is no device capacity that is exceeded in other case scenarios. When comparing the maximum and minimum fault currents in each of the busses investigated with respect to the cases, no great differences can be found.

Table 3. Short circuit analysis result.

Bus ID	Case 0		Case 1-1		Case 1-2		Case 2-1		Case 2-2	
	Max (rms kA)	Min (rms kA)	Max (rms kA)	Min (rms kA)	Max (rms kA)	Min (rms kA)	Max (rms kA)	Min (rms kA)	Max (rms kA)	Min (rms kA)
Bus 4	34.627	30.092	34.630	30.092	36.643	30.116	34.631	30.092	34.654	30.121
Bus 5	35.292	30.118	37.038	30.118	46.836	37.957	35.296	30.118	35.319	30.147
Bus 6	31.327	26.871	31.327	26.871	31.327	26.871	31.327	26.871	31.327	26.871
Bus 8	32.051	26.953	32.051	26.953	32.051	26.953	32.051	26.953	32.051	26.953
Bus 1	196.950	156.084	197.345	156.084	199.034	158.059	197.497	156.084	200.569	158.542
Bus 7	196.922	156.089	196.922	156.089	196.922	156.089	196.922	156.089	196.922	156.089

3.3. Relay Coordination Study Result

The overcurrent relays (OCRs) coordinated under phase fault conditions were analyzed using the ETAP's star view [25]. With the proper relay settings, the circuit breakers near to the primary fault trip off first to ensure its selectivity characteristic. The sequence of operation (SoP) for the relays was simulated when a three-phase fault occurred at bus 4, bus 5 and bus 1. Table 4 shows the SoP events in each case scenario. From the table, in case 1-2, the SoP when a three-phase fault occurs at bus 4 can be seen not to conform to the sequence in other cases. This was as a result of the case having the highest maximum fault current of 36.643 kA with bus 5 at the highest maximum fault current of 46.836 kA

(refer to Table 3). The corresponding circuit breaker with a maximum interrupting capability (40 kA) is low at bus 5. Thus, CB3 needs to be changed to a much higher value to accommodate for a fault when it occurs. CB2 and CB3 are the circuit breaker identification names. The assignment of the circuit breakers trip order is summarized in Table 5.

Table 4. Sequence of operation events.

Bus ID	Case 0	Case 1-1	Case 1-2	Case 2-1	Case 2-2
Bus 4	A	A	C	A	A
Bus 5	B	B	B	B	B
Bus 1	C	C	C	C	C

Table 5. Circuit breaker trip order assignment.

Circuit Breaker Trip Sequence	A	B	C
First Trip	CB2	CB3	CB2
Second Trip	CB2	CB3	CB3
Third Trip	CB3	CB2	CB2

The one-line diagrams for the SoPS of each fault location for bus 4, bus 5 and bus 1, respectively, are shown in Figures 8–10.

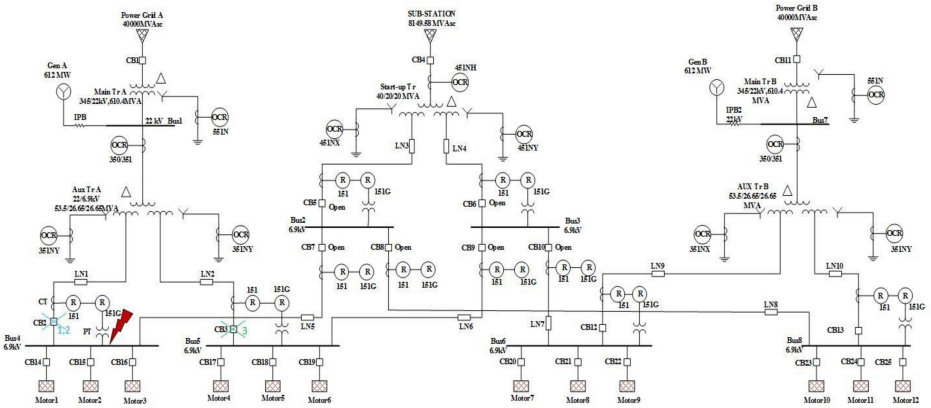

Figure 8. Fault at bus 4.

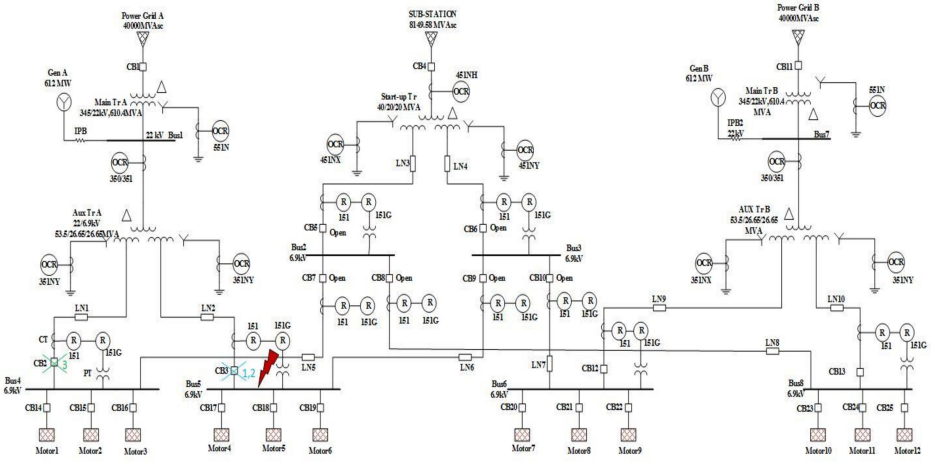

Figure 9. Fault at bus 5.

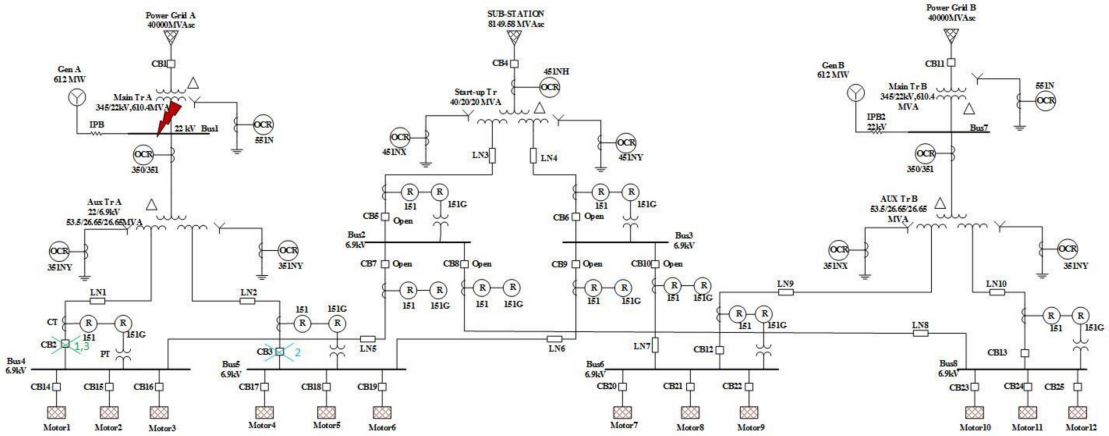

Figure 10. Fault at bus 1.

With ETAP software's star view, the circuit breakers' operating sequence reports can be obtained. In this paper, a sample of the report when a symmetrical three-phase fault occurs at bus 4 is obtained, as shown in Figure 8. This sequence of operation event report in Table 6 clearly indicates the time at which the fault occurred, the fault current and the relay which senses the signal and causes the circuit breaker to trip off. The auxiliary transformer (high voltage) is denoted (Aux Tr_HV) and the transmission line is denoted (LN).

Table 6. Sequence of operation reports for faults at bus 4.

Symmetrical Three-Phase Fault at Bus 4				
Time (ms)	**ID**	**Fault Current (kA)**	**T1 (ms)**	**Condition**
7.2	350/351 (Aux TR_ HV)B	9.047	2.6	Phase-OC1-50
20.0	151(LN1)	29.041	<20.0	Phase-OC1-51
82.7	151N(LN1)	29.041	<82.7	Phase-OC1-51
101	350/351 (Aux TR_HV)B	9.047	101	Phase-OC1-51
103	CB2		83.3	Tripped by 151(LN1) Phase-OC1-51
166	CB2		83.3	Tripped by 151N(LN1) Phase-OC1-51
217	151N(LN2)	0.197	217	Phase-OC1-51
300	CB3		83.3	Tripped by 151N(LN2) Phase-OC1-51
572	151(LN2)	0.197	572	Phase-OC1-51
655	CB3		83.3	Tripped by 151(LN2) Phase-OC1-51

The coordinated curves for phase faults according to the overcurrent relay (151 and 151N) settings are shown in Figure 11a. The normalized TCC graph for a fault at bus 4 is shown in Figure 11b, indicating that the fault current at this instant is 29.041 kA.

3.4. Cost Estimate Evaluation

The cost evaluation for an additional substation facility with ultra-high voltage was performed to compare the ESS locations in the power plant. Substation cost estimates were evaluated for equipment, protection and control at 69 kV, 230 kV and 345 kV voltage levels. It can be verified from Table 7 that the cost of an additional substation at the 345 kV section will incur an estimate cost of about $1,018,168 for the selected equipment. Thus, there is a huge difference when comparing the cost estimates for 22 kV and 6.9 kV, which are low voltage, to 69 kV, with an estimate cost of $299,689. Therefore, position 3 was excluded in the feasibility analysis of ESS integration.

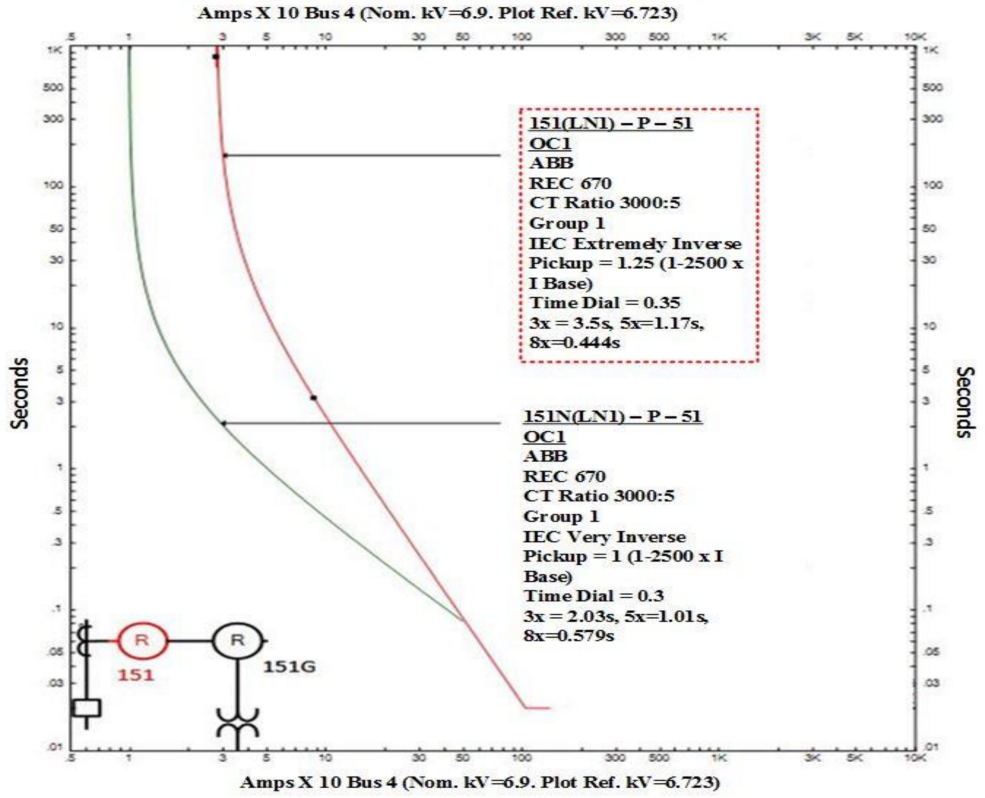

(**a**)

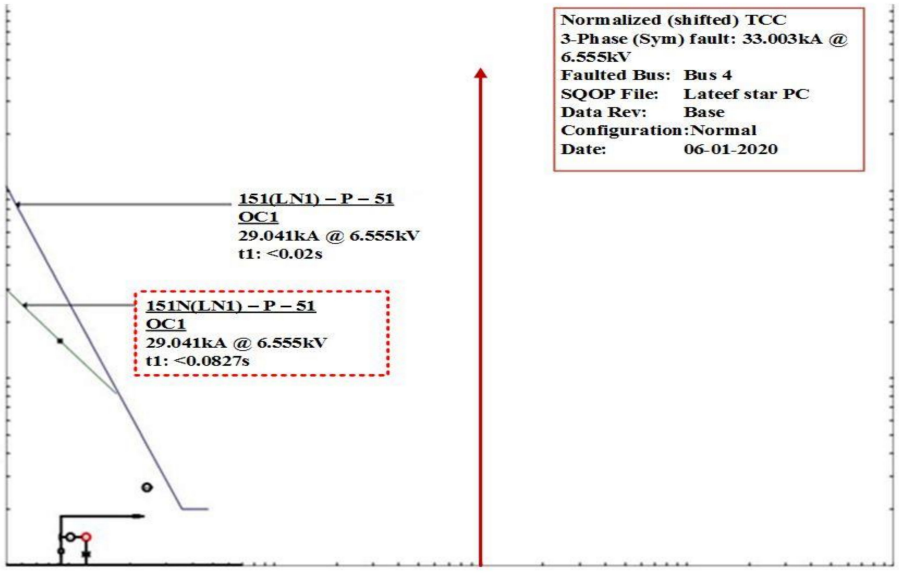

(b)

Figure 11. OCR 151 and 151N. (**a**) time current curves (TCCs) for a phase fault; (**b**) normalized TCC.

Table 7. Substation cost estimate evaluation [26].

Voltage Level	Circuit Breakers ($)	Voltage Transformer ($)	Current Transformer ($)	Bus & Fittings ($)	Power Transformer ($/MVA)	Relay Panel ($)	Total Cost ($)
69 kV	67,116	65,022	85,266	21,312	4720	56,250	299,686
230 kV	134,680	112,327	170,979	38,764	7110	109,500	573,360
345 kV	388,928	141,663	282,463	50,194	8670	146,250	1,018,168

4. Conclusions

In this paper, a method of carrying out a feasibility study for the installation of an ESS in a power system based on the case scenarios is proposed. To verify the proposed method, the ESS and load were modeled, and an analysis simulation was performed. The estimated cost of the selected ESS locations was evaluated, and the 345 kV voltage level was excluded from the analysis. The result from the load flow studies for each case scenario showed that the overloading of equipment (auxiliary transformer) occurred at bus 5 with a percentage loading of 117.5% when the load ESS was installed at the lower-voltage (6.9 kV) level (case 1-1) in the power system, which could damage the equipment. The study also revealed that no voltage violation occurred in all cases as the rated nominal was within the operating range of 90%~100%, as expected. Short circuit analysis results showed that, expect for case 1-2, in which the maximum fault current exceeded the device capacity at fault on bus 5, there were no great differences for both sub-transient and steady state fault currents in other cases. The relay coordination study, however, showed a similar sequence of operation events of the circuit breaker tipping in all cases except for case 1-2, which was due to the short circuit fault current exceeding the device. Thus, the results obtained from the feasibility studies of the power system showed that the most appropriate location to install the ESS was on the upper voltage level of 22 kV (Case 2-1 and 2-2), which had neither a load flow, voltage violation nor fault current that exceeded the device capacity in these cases.

Based on this study, it is expected that the proposed method necessitates technological development, whereby a plant facility with a high level of safety could be ensured when an ESS is integrated. Our work also validates the Gen-FR of an ESS through system analysis.

Author Contributions: Conceptualization, L.O.I. and M.Y.; Investigation, M.Y. and D.H.; Methodology, L.O.I. and M.Y.; Supervision, M.Y. and Y.-M.S.; Writing—original draft, L.O.I.; Review and manuscript approval; L.O.I., Y.-M.S., D.H. and M.Y. All authors have read and agreed to the published version of the manuscript.

Funding: This work was supported by the Korea Institute of Energy Technology Evaluation and Planning (KETEP) and the Ministry of Trade, Industry & Energy (MOTIE) of the Republic of Korea (No. 20182410105330) and National Research Foundation Grant (No. 2020R1F1A1076638) funded by the Korean government.

Acknowledgments: This work was supported by the Korea Institute of Energy Technology Evaluation and Planning (KETEP) and the Ministry of Trade, Industry & Energy (MOTIE) of the Republic of Korea (No. 20182410105330) and National Research Foundation Grant (No. 2020R1F1A1076638) funded by the Korean government.

Conflicts of Interest: The authors declare no conflict of interest.

References

1. Wade, N.; Taylor, P.; Lang, P.; Jones, P. Evaluating the benefits of an electrical energy storage system in a future smart grid. *Energy Policy* **2010**, *38*, 7180–7188. [CrossRef]
2. Bolufawi, O. Renewable Energy Integration with Energy Storage Systems and Safety. In *Special Topics in Renewable Energy Systems*; IntechOpen: London, UK, 2018; p. 39.
3. Kousksou, T.; Bruel, P.; Jamil, A.; El Rhafiki, T.; Zeraouli, Y. Energy storage: Applications and challenges. *Sol. Energy Mater. Sol. Cells* **2014**, *120*, 59–80. [CrossRef]
4. Gür, T.M. Review of electrical energy storage technologies, materials and systems: challenges and prospects for large-scale grid storage. *Energy Environ. Sci.* **2018**, *11*, 2696–2767. [CrossRef]
5. Swaminathan, S.; Sen, R. *Review of power quality applications of energy storage systems. Review of Power Quality Applications of Energy Storage Systems*; Sandia National Labs.: Albuquerque, NM, USA, 1997. [CrossRef]
6. Mundackal, J.; Varghese, A.C.; Sreekala, P.; Reshmi, V. Grid power quality improvement and battery energy storage in wind energy systems. In Proceedings of the 2013 Annual International Conference on Emerging Research Areas and 2013 International Conference on Microelectronics, Communications and Renewable Energy, Kanjirapally, India, 4–6 June 2013; pp. 1–6.

7. Sels, T.; Dragu, C.; Van Craenenbroeck, T.; Belmans, R. Overview of new energy storage systems for an improved power quality and load managing on distribution level. In *16th International Conference and Exhibition on Electricity Distribution (CIRED 2001)*; Institution of Engineering and Technology (IET): London, UK, 2001.
8. Shin, S.-S.; Oh, J.-S.; Jang, S.-H.; Cha, J.-H.; Kim, J.-E. Active and Reactive Power Control of ESS in Distribution System for Improvement of Power Smoothing Control. *J. Electr. Eng. Technol.* **2017**, *12*, 1007–1015. [CrossRef]
9. Barelli, L.; Bidini, G.; Pelosi, D.; Ciupageanu, D.; Cardelli, E.; Castellini, S.; Lăzăroiu, G. Comparative analysis of AC and DC bus configurations for flywheel-battery HESS integration in residential micro-grids. *Energy* **2020**, *204*, 117939. [CrossRef]
10. Bazargan, D. A Study of Battery Energy Storage Dynamics in Power Systems. Ph.D. Thesis, University of Manitoba, Winnipeg, MB, Canada, 2014.
11. Ciupageanu, D.-A.; Barelli, L.; Lazaroiu, G. Real-time stochastic power management strategies in hybrid renewable energy systems: A review of key applications and perspectives. *Electr. Power Syst. Res.* **2020**, *187*, 106497. [CrossRef]
12. Emadi, A.; Khaligh, A.; Rivetta, C.; Williamson, G. Constant Power Loads and Negative Impedance Instability in Automotive Systems: Definition, Modeling, Stability, and Control of Power Electronic Converters and Motor Drives. *IEEE Trans. Veh. Technol.* **2006**, *55*, 1112–1125. [CrossRef]
13. Devdhariya, M.D.; Adroja, V.R.; Rafaliya, K.M.; Desai, M.M. Power System Protection with Relay Co-ordination. *Int. J. Eng. Dev. Res.* **2017**, *5*, 101–105.
14. Homburg, K.A. *Short-Circuit, Coordination, and Arc-Flash Studies for Data Centers: Best Practices and Pitfalls*; Schneider Electric: Former residence, Luet, France, 2010.
15. Relay Coordination Study and Analysis. Available online: https://carelabz.com/relay-coordination-study-and-analysis/ (accessed on 8 October 2019).
16. Kusekwa, M.A. Load Flow Solution of the Tanzanian Power Network Using Newton-Raphson Method and MATLAB Software. *Int. J. Energy Power Eng.* **2014**, *3*, 277. [CrossRef]
17. Husain, T.; Khan, M.; Ansari, M. Power Flow Analysis of Distribution System. *Int. J. Adv. Res. Electr. Electron. Instrum. Eng.* **2016**, *5*, 4058–4065.
18. Load Flow —Step by Step. Available online: https://electrisim.com/load-flow-power-flow.html (accessed on 17 September 2019).
19. Raj, P. Load Flow and Short Circuit Analysis of 400/220 kV Substation. *Int. J. Creat. Res. Thoughts* **2013**, *1*, 1–4.
20. Zeggai, A.; Benhamida, F. Power Flow and Short Circuit of 220 kV Substation using ETAP. In Proceedings of the 2019 Algerian Large Electrical Network Conference (CAGRE), Algiers, Algeria, 26–28 February 2019.
21. Bangash, K.N.; Farrag, M.E.A.; Osman, A.H. Impact of Energy Storage Systems on the Management of Fault Current at LV Network with High Penetration of Distributed Generation. *Int. J. Smart Grid Clean Energy* **2017**, *6*, 195–206. [CrossRef]
22. Al-Nussairi, M.K.; Bayindir, R.; Padmanaban, S.; Mihet-Popa, L.; Siano, P. Constant Power Loads (CPL) with Microgrids: Problem Definition, Stability Analysis and Compensation Techniques. *Energies* **2017**, *10*, 1656. [CrossRef]
23. Ram, S.S.; Daram, S.B.; Venkataramu, P.S.; Nagaraj, M.S. Analysis of ZIP Load Modeling in Power Transmission System. *Int. J. Control. Autom.* **2018**, *11*, 11–24. [CrossRef]
24. Yoon, M.; Lee, J.; Song, S.; Yoo, Y.; Jang, G.; Jung, S.; Hwang, S. Utilization of Energy Storage System for Frequency Regulation in Large-Scale Transmission System. *Energies* **2019**, *12*, 3898. [CrossRef]
25. Electrical Transient Analyzer Program (ETAP). *Training Manual*; ETAP: Irvine, CA, USA, 2014.
26. Transmission Cost Estimation Guide for MTEP 2019. Available online: https://cdn.misoenergy.org/20190212%20PSC%20Item%2005a%20Transmission%20Cost%20Estimation%20Guide%20for%20MTEP%202019_for%20review317692.pdf (accessed on 2 October 2020).